Published in final edited form as:
Dev Dyn. 2008 June ; 237(6): 1746–1753. doi:10.1002/dvdy.21572.

Cardiac expression patterns of endothelin-converting enzyme (ECE): Implications for conduction system development

David Sedmera[1,3,4], **Brett S. Harris**[1], **Elizabeth Grant**[1], **Ning Zhang**[1], **Jane Jourdan**[1], **Dana Kurkova**[3], and **Robert G. Gourdie**[1,2]

[1]Department of Cell Biology and Anatomy, Medical University of South Carolina

[2]Pediatric Cardiology Medical University of South Carolina

[3]Institute of Anatomy, First Faculty of Medicine, Charles University, Prague

[4]Institute of Animal Physiology and Genetics, Academy of Sciences of the Czech Republic

Abstract

The spatiotemporal distribution of the endothelin-converting enzyme (ECE) protein in the embryonic chick heart and the association of this polypeptide with developing cardiac conduction system is described here for the first time. Further, we show how cardiac hemodynamic load directly affects ECE level and distribution. Endothelin (ET) is a cytokine involved in the inductive recruitment of Purkinje fibers. ET is produced by proteolytic cleavage of Big-ET by ECE. We generated an antibody against chick ECE recognizing a single band at ~70 kD to correlate the cardiac expression of this protein with that reported previously for its mRNA. ECE protein expression was more widespread compared to its mRNA, being present in endothelial cells, mesenchymal cells and myocytes, and particularly enriched in the trabeculae and nascent ventricular conduction system. The myocardial expression was significantly modified under experimentally altered hemodynamic loading. In vivo, ET receptor blockade with bosentan delayed activation sequence maturation. These data support a role for ECE in avian cardiac conduction system differentiation and maturation.

Keywords

chick embryo; heart development; immunohistochemistry; endothelin signaling; ventricular conduction system; Purkinje fibers; bosentan

Introduction

Endothelin-1 (ET-1) is a 21-amino-acid peptide that has potent vasoconstrictor activity (Yanagisawa et al., 1988; Braunwald et al., 2001). Two further isoforms of endothelin have been described (ET-2 and ET-3), but endothelium produces only ET-1. Synthesis of ET-1 is complex, starting with a large precursor molecule, preproendothelin, which is proteolytically cleaved to “big endothelin” (Big-ET) . Big-ET is in turn converted by the specific peptidase activity of the endothelin-converting enzyme (ECE) to fully active ET-1. In vascular tissues, ET-1 is synthesized in endothelium and secreted on the abluminal side of the vascular wall, acting as an autocrine or paracrine signaling molecule. Although active ET is present in circulation, and its levels are increased in patients with heart failure, the half-life of ET is

Correspondence to: Robert G. Gourdie, Department of Cell Biology and Anatomy, Medical University of South Carolina, 173 Ashley Avenue, BSB 601, Charleston, SC 29425, Phone: 1-843-792-8181, Fax: 1-843-792-0664, E-mail: gourdier@musc.edu.

only a few minutes because of rapid clearance by the lung; therefore, ET is considered an autocrine or paracrine cytokine, not a hormone.

Endothelin signaling mediated via ETA receptor is essential for normal embryonic patterning in birds (Kempf et al., 1998) and mammals (Kurihara et al., 1994; Kurihara et al., 1995; Kurihara et al., 1997; Yanagisawa et al., 1998a). In both classes of vertebrates, targeting of this pathway leads to effects on cranio-facial neural crest derivatives and also cardiovascular defects. Indeed, ventricular septal defects were noted in 48% of ET-1-null mice (Kurihara et al., 1995), and this frequency increased up to 90% with an additional ETA antagonist treatment. Cardiovascular defects in this latter sub-group included reductions in trabeculation and loss of muscle and fibrous tissues at the crest of the interventricular septum – a location in heart rich in conduction system tissues. Similar basal/crestal defects to the interventricular septum have been noted in double knockouts in mice of genes encoding ECE-1 and ECE-2, the enzymes responsible for activation of big-ET (Yanagisawa et al., 1998b).

There is evidence that exogenously administered ET can induce expression of CCS markers in embryonic chick and mouse cardiomyocytes *in vitro* (Gourdie et al., 1998). Treatment of embryonic stem cells from mouse with exogenous ET, but not neuregulin results in upregulation of markers of CCS phenotype, including the gap junction proteins Cx40 and Cx45 (Gassanov et al., 2004). In further work in the chick embryo it was shown that overlapping ectopic expression of human big ET-1 and bovine ECE-1 induced ectopic conduction tissues *in vivo* (Takebayashi-Suzuki et al., 2000). More recently we have demonstrated that hemodynamically-induced up-regulation of ECE correlates with precocious differentiation of ventricular CCS in the chick model (Reckova et al., 2003; Hall et al., 2004). Direct evidence that active ET is sufficient to induce specialized cardiac tissues is thus mounting. However, as yet there has been no direct demonstration that ET signaling is necessary for the differentiation of vertebrate CCS cells in vivo.

All reports thus far have only shown ECE expression at the mRNA level, since production of antibody probes against this peptidase has proven difficult. Based on a strategy developed by Ergul and co-workers (Jafri and Ergul, 2003) we have successfully developed a specific antibody to chick ECE-1. In this study, we use this antibody to probe cardiac distribution patterns of ECE in the chick embryonic heart at the protein level and correlate this expression with sites of conduction system formation. Using the same custom antibody, we further show protein changes under experimentally altered hemodynamic conditions. Finally, chronic administration of the ET dual receptor antagonist bosentan resulted in delay in ventricular CCS maturation. Together, these data indicate a role for ET signaling in CCS induction during normal development of the chick *in vivo*.

Results

Antibody characterization and expression pattern

The raising of antibodies to ECE protein has proven to be difficult. Inspired by our colleague at the Medical College of Georgia, Dr Ergul, who successfully raised an antibody against porcine ECE (Jafri and Ergul, 2003), we used a 15 amino acid peptide (plgspmnppkkcevw) from the carboxyl-terminus of chick ECE-1 (which differs by one amino acid residue from its porcine homologue) to develop a custom polyclonal antibody in rabbit. Consistent with the predicted molecular mass of chick ECE-1, the antibody localized a single ~70 kD molecular mass band on Western blots of chick embryonic heart homogenates (Figure 1).

We next proceeded to assess developmental changes in ECE expression in the chick embryonic heart. While the antibody bound to endocardial and coronary artery endothelial tissues in embryonic chick heart as expected from its published mRNA localization (Takebayashi-Suzuki et al., 2000), we found other aspects of the ECE-1 expression patterns that were not evident in the previous in situ hybridization studies (Figure 2). While the ECE protein intensely labeled endothelial and endocardial cells prior to embryonic day 6 (E6, Stage 29) with the most intense staining in the endocardium covering the valves, i.e., region exposed to high shear stress as expected, the protein was also detectable in myocardial tissues. Importantly, this myocardial expression became increasingly restricted to, and up-regulated in CCS tissues, including the bundle branches, subendocardial and periarterial Purkinje fibers, as confirmed by PSA-NCAM and connexin40 immunostaining (Figure 2). Simultaneously with its up-regulation in CCS tissues, there was an apparent down-regulation of ECE in endothelial cells covering the trabeculae. The timing of this transition from endothelial to myocardial expression of ECE was auspicious, as it corresponded to the time course in which we have previously characterized ongoing recruitment into CCS lineages (Cheng et al., 1999).

The myocardial expression showed a clear gradient, with enrichment in the forming conduction tissues such as periarterial Purkinje fibers (Figures 3, 4) tapering off into the surrounding working myocardium. At post-hatching stages, restriction to CCS became complete with virtually no expression persisting in the working ventricular myocardium.

Changes in ECE protein levels under altered hemodynamic conditions

Previous studies (Hall et al., 2004; Sedmera et al., 2004) have shown that cardiac ECE mRNA is up-regulated in response to increased hemodynamic loading and down-regulated by decreases in this mechanical input. We next set to verify the biological validity of these changes at the protein level, using a well-established method of quantifying fluorescent signal from immunostained sections (Sedmera et al., 2002; Harris et al., 2006). This approach is better suited to quantify regional changes in protein expression within millimeter-sized hearts. Using a chick model of left heart hypoplasia (Sedmera et al., 2002), quantitative immunofluorescence enabled discrimination of a down-regulation of ECE in the relatively unloaded, hypoplastic left ventricle of the model and a corresponding up-regulation of ECE in the compensating right ventricle (Figure 5).

Inhibition of ET signaling prevents CCS maturation

To test functionally the physiological role of ET signaling in CCS development, we performed *in ovo* experiments involving treatment with the broad-spectrum ET receptor antagonist bosentan. First, we examined the physiological effect of targeting ET receptors by probing for the presence or absence of anterior septal branch (ASB), also known as a part of putative primary ring (de Groot et al., 1987; Wessels et al., 1996). In the anterior view, ventricular activation via this pathway at HH21 (E4) is considered as an “early” hallmark of CCS maturation (Sedmera et al., 2004). In 11 HH17 (E3) embryos, 10 showed immature base-to-apex, left-to-right (i.e. along blood flow) ventricular activation, while in 17 HH21 embryos, 15 demonstrated the more mature ASB activation. However, bosentan treatment at E2 and E3 only resulted in a mild, non-significant decrease in the ASB pattern (positive in 14/19 embryos, $p=0.23$ vs. HH21 controls). Thus, while inhibition of ET receptors suggested a trend toward decreasing the maturity of activation in the E2/3 chick heart, no obvious effects on conduction system differentiation were observed.

Next, we examined the effect of chronic bosentan treatment between E2-E8 during which time the ventricular activation undergoes a definitive switch from a base-to-apex to apex-to-base sequence. Progression to apex-first activation provides a definitive and sensitive

functional marker of maturation of the ventricular conduction system in chick (Chuck et al., 1997; Reckova et al., 2003; Hall et al., 2004; Gurjarpadhye et al., 2007). Optical mapping performed in a pilot series of experiments (n=17) at E8 showed a significant decrease in proportion of hearts with functionally mature (apex-to-base) activation pattern compared to vehicle-treated controls (p=0.006). No difference between these controls and intact embryos from our previous study (Reckova et al., 2003) was noted. In addition, in bosentan-treated embryos, the few which did show apex-to-base activation, the site of the first breakthrough was on the left side, in contrast to controls, which showed right-sided breakthrough, indicating functionality of the right bundle branch. These results were further corroborated by a second series of experiments, where optical mapping was performed at E8 and E9 (Stages 34 and 35). Quantification of the angular position of the epicardial breakthrough site according to a recently published protocol (Gurjarpadhye et al., 2007) at both stages demonstrated a significant shift towards immature patterns (Figure 6): 120 reduced to 80 degrees and 120 reduced to 60 degrees at E8 and E9 respectively, consistent with an absence or delay of ventricular CCS maturation. We concluded that blockade of ET signaling was sufficient to inhibit functional maturation of the ventricular CCS *in ovo*.

Given the abnormal function of the ventricular CCS, we next sought to determine whether there were correlated morphological substrates. Staining for very early markers of developing avian CCS (e.g., loss of HNK1, PSA-NCAM) as well as routine histology (hematoxylin and eosin) did not reveal any differences between control and bosentan-treated embryos at E8 or E9. However, these early markers precede expression of definitive morphological markers of the CCS such as Cx40, which are expressed later during incubation *in ovo*. We thus extended the bi-daily bosentan treatment until E15 to assess formation of subendocardial and periarterial Purkinje fibers with connexin40 immunohistochemistry. Unfortunately, survival of bosentan-treated embryos to this time point was only 15%, and though Purkinje fibers could be visualized by connexin40 and ECE expression within this cohort (Figure 3), the high death rates resulting from this experiment precluded us from drawing conclusions at this time.

Discussion

Avian conduction cells are characterized by a precise and spatially restricted differentiation corresponding to just a few cell layers, i.e., periarterially, subendocardially, and around central conduction bundles. If ET-1 is indeed involved in conduction cell differentiation *in vivo* (Pennisi et al., 2002; Gourdie et al., 2003), short-range autocrine or paracrine mechanisms reinforcing the restricted differentiation patterns initiated by this potent and potentially long-range factor would seem probable. In the bird, there is strong evidence for a process of conscription of multipotent progenitor cells to both central and peripheral elements of the developing conduction system (Gourdie et al., 1995; Cheng et al., 1999). The best evidence for this comes from studies of the developmental relationship between conduction cells and vascular tissues in the chick embryo (reviewed in Gourdie et al., 2003). In this species, the most terminal Purkinje fibers of the conduction system co-distribute and ramify intimately with coronary arteries. By using replication-defective retroviruses, it was found that myocytes infected in the avian tubular heart continued to be capable of differentiating into conduction cell fates around the coronary arteries until close to hatching (Gourdie et al., 1995).

The localization pattern of ECE protein shown in this study is consistent with the above hypothesis, further strengthening the case for ECE as a hemodynamic sensor in the events leading to differentiation of CCS from cardiomyogenic progenitors. In particular, the early enrichment of ECE in nascent conduction tissues, appears to be well-suited for generating a localized concentration of active ligand necessary for the proposed role of ET-1 in inducing

CCS phenotype. In addition to ECE mRNA expression in endocardium, expression in cushion mesenchyme, but not myocardium, has been reported in chick during cardiac development (Takebayashi-Suzuki et al., 2000; Hall et al., 2004). The apparent failure to detect myocardial expression of mRNA in previous *in situ* hybridization reports may be due to suboptimal probe penetration at later developmental stages, since there is evidence that ECE is highly expressed as detected by both mRNA and protein in mammalian myocardial cells (Ergul et al., 2000; Pikkarainen et al., 2006). More over, the spatially restricted myocardial distribution of ECE, also correlates with the expression patterns of the ET receptors, ETA and ETB (Takebayashi-Suzuki et al., 2000). While ETA mRNA shows a homogeneous expression throughout the myocardium of the avian embryo, ETB is expressed preferentially (although not exclusively) in atrial myocardium and in the ventricular subendocardium.

The utility of this novel antibody generated against chick ECE was demonstrated on the experimental left heart hypoplasia model. In agreement with previously reported changes at the mRNA level (Hall et al., 2004; Sedmera et al., 2004), there was a decrease in the hypoplastic left ventricle and an increase in the compensating right ventricle. Importantly, these changes in ECE expression are linked to a physiological phenotype assessed by optical mapping, interpreted as a delay of CCS functional maturation (Reckova et al., 2003). The chick ECE antibody appeared to show cross reactivity in mouse heart, revealing a staining pattern for presumptive ECE-1 (enrichment in the endocardium, atrioventricular valves, conduction system – Supplemental Figure 1) similar to that observed in the embryonic chicken heart. This cross reactivity is perhaps to be expected as the 15 amino acid peptide epitope used to raise the antibody differed by only a single conservative amino acid change from a corresponding CT peptide in mammal. Thus, at appropriate stages, this antibody may have utility as an immunohistochemical marker of the developing CCS.

The fact that CCS function was blocked by ET receptor antagonist bosentan raises an interesting parallel with a recently published study on the effects of neural crest ablation on conduction system development (Gurjarpadhye et al., 2007). In both the aforementioned and current study, an identical method (optical mapping with angle value measurement) was used, and the electrophysiological phenotype was similar. Physiologically, the apical breakthrough appears first on the right side, correlating with the earlier maturation of the right bundle branch. Conduction through the right bundle branch was also found to be a more sensitive marker of conduction disturbances in connexin40 null mouse (Tamaddon et al., 2000). Activation from the left side between ED7-9 corresponds with earlier immature base-to-apex activation. This was quantified in the second series of experiments, performed after the clock-face semi-quantitative evaluation of ventricular activation patterns had been described and validated by Gurjarpadhye et al. (2007). Unlike in the neural crest ablated hearts, no morphological anomalies of the CCS tissues (examined by conventional histology and HNK1 and PSA-NCAM antibodies) were observed (data not shown). According to the original description of bosentan effects on chick embryo (Kempf et al., 1998), the target of its teratogenic mechanism is the ETA receptor expressed by the neural crest cells. This correlated with deficiencies of the facial structures (micrognathia was a constant finding in our series, conveniently serving as a positive control for the phenotype). However, in contrast to the above study we did not observe ventricular septal defects in any of the 16 hearts examined histologically, and also heart size (as assessed from en face view) appeared normal. ET requirement for neural crest cells differentiation seems conserved among vertebrates, as attested by a recent paper showing importance of ET-ETA signaling in facial skeletal patterning in the zebrafish (Nair et al., 2007).

In conclusion, we have generated a novel antibody against chick ECE and demonstrate that protein level expression patterns are distinct from its mRNA, but consistent with the

physiological role of ET signaling in avian CCS formation. It remains to be shown whether ET signaling is implicated in CCS development also in mammals.

Experimental Procedures

Antibody production

We used a 15 amino acid peptide (plgspmnppkkcevw) from the CT of chick ECE-1 (which differs by one amino acid residue from its mammalian homologue) to develop a custom polyclonal antibody in rabbit using a commercial service provided by Research Genetics Inc., AL.

Western blotting

Embryonic hearts were excised, trimmed, and rinsed in cold physiological saline, and then minced, rinsed again, and snap-frozen at −80 °C. Frozen samples were homogenized in 0.5ml homogenization buffer (50mMTris-HCl pH 7.5, 2% SDS, 0.5% sodium deoxycholate, 0.25M sucrose, 10mM EGTA, 4mM EDTA, 1mM sodium orthovanadate, 1mM NaF, Sigma protease inhibitors) and syringed using a 22 gauge needle followed by a 26 1/2-gauge needle. The homogenates were centrifuged at 7000 × g for 10 minutes at 4 °C. Total protein content was determined by the Bradford method (Bio-Rad, DC) using bovine serum albumin as a standard. Western blotting was carried out using methods similar to those described previously (Hewett et al., 2005; Hunter et al., 2005; Harris et al., 2006). In brief, 30 micrograms of total protein was subjected to SDS-PAGE (Bio-Rad 4-20% Tris-HCL) and transferred to Immobilon P (Millipore) filters. The filters were probed with the cECE-1 polyclonal antibody 1:1000, and developed using chemiluminescence CDP STAR substrate (Tropix Applied Biosystems). The membranes were stripped, re-probed with mouse GAPDH 1:8500 (RDI), and developed again with CDP STAR.

Immunohistochemistry

Serial dilutions from 1:1 to 1:1000 were tested on frozen sections (paraformaldehyde-fixed) and on paraffin sections (fixed in either 4% paraformaldehyde in PBS overnight at 4 °C or with 80% methanol – 20% dimethylsulfoxide for at least 24 h at room temperature). Optimal dilution determined empirically for fluorescent secondary detection was 1:50 for paraffin sections and 1:100 for frozen sections, although signal was detectable at 1:200 and 1:500 dilutions, respectively. Both fixatives used for paraffin sections worked to satisfaction, with paraformaldehyde showing slightly higher background. Specificity of antibody labeling was controlled for by multiple means: using Cy5-compled secondary to minimize contribution of endogenous fluorescence, incubation with pre-immune rabbit serum, omission of primary antibody, or its pre-absorption by the peptide against which it was raised. All negative controls showed staining intensity at least ten times lower than the specific signal (see Figures 2 and 3 for examples). The images for presentation were obtained by blocking and permeabilization with 1% bovine serum albumin and 0.1% Triton-X in TBS for 2 hours followed by overnight incubation with the primary antibody at room temperature (1:50 for paraffin sections showed in Figure 2, or 1:100 for frozen sections showed in Figure 3, diluted in the blocking buffer), rinsing, and 4 h incubation with Cy3-coupled anti-rabbit secondary antibody (Jackson Immuno). For tissue contrast, tissue autofluorescence was recorded at Leica TCS SP2 AOBS confocal microscope in the fluorescein channel (488 nm blue excitation) and specific fluorescence in sequential mode by green excitation at 543 nm. The images were processed in Adobe Photoshop; no further background subtraction or filtering was used, and identical exposure settings optimized for positive signal during acquisition were used for negative controls. In total, over 100 hearts at stages between ED4-100 days post-hatching were analyzed, with a minimum of 3 hearts per stage.

Experimental changes in hemodynamic loading

Left atrial ligation (to induce volume underload in the left ventricle and overload in the right ventricle) were performed as described previously (Sedmera et al., 1999; Reckova et al., 2003). For quantitative immunofluorescence, performed as described above and previously (Sedmera et al., 2002), sister sections from control and hypoplastic hearts generated in the context of previous studies (Reckova et al., 2003; deAlmeida et al., 2007) were stained as described above, including the negative controls.

In ovo bosentan treatment

In the pilot series with bosentan free base, we used 30 μl of olive oil suspension (5 mg/ml) applied over the embryo according to published protocol (Kempf et al., 1998). However, the results obtained by this approach were not consistent, there was variable amount of insoluble residue, and the facial phenotype was not completely penetrant, suggesting lack of uniform distribution. We then switched to use of water-soluble sodium salt, and found as an optimal compromise between phenotype penetrance and survival repeated dosing of 250 μg dissolved in 200 μl of distilled water, applied through the air space directly over the embryo at E2, 4, 6, and 8. With this protocol, survival until E9 was around 30%, with about 50% mortality occurring prior to E4.

Vehicle-treated and experimental embryos were sampled at E8 (Hamburger-Hamilton Stage 34, (Hamburger and Hamilton, 1951) or E9 (Stage 35). The hearts were dissected out of the embryos and stained with di-4-ANEPPS (Invitrogen). For imaging, they were pinned on the bottom of Sylgard-lined dish filled with oxygenated Tyrode's-HEPES buffer (pH 7.4, 37 °C). Optical mapping was performed on an Olympus BX51WI fixed-stage upright fluorescence microscope fitted with temperature-controlled stage and ULTIMA-L high-speed camera (SciMedia, Japan). The setup and data processing (BV_Analyzer software, bundled with the camera) does not differ substantially from our previous descriptions (Reckova et al., 2003). Analysis and interpretation was performed exactly as described in detail recently (Gurjarpadhye et al., 2007).

Supplementary Material

Refer to Web version on PubMed Central for supplementary material.

Acknowledgments

Supported by NIH RR16434, NIH HL082802, NIH HL56728, MSMT VZ 206100-3, AS CR AVOZ50450515, and GACR 304/08/0915. D. S. is also supported by the Purkinje Fellowship of the Academy of Sciences of the Czech Republic. B.S.H. was supported by 5P20RR016434-07 from the NCRR. Bosentan was kindly provided by Dr. Martine Clozel (Actelion Pharmaceuticals).

References

Braunwald, E.; Zipes, DP.; Libbt, P. Heart Disease: A Textbook of Cardiovascular Medicine. Philadelphia: Saunders; 2001. p. 2281

Cheng G, Litchenberg WH, Cole GJ, Mikawa T, Thompson RP, Gourdie RG. Development of the cardiac conduction system involves recruitment within a multipotent cardiomyogenic lineage. Development. 1999; 126:5041–5049. [PubMed: 10529421]

Chuck ET, Freeman DM, Watanabe M, Rosenbaum DS. Changing activation sequence in the embryonic chick heart. Implications for the development of the His-Purkinje system. Circ Res. 1997; 81:470–476. [PubMed: 9314827]

de Groot IJ, Sanders E, Visser SD, Lamers WH, de Jong F, Los JA, Moorman AF. Isomyosin expression in developing chicken atria: a marker for the development of conductive tissue? Anat Embryol. 1987; 176:515–523. [PubMed: 3318555]

deAlmeida A, McQuinn T, Sedmera D. Increased ventricular preload is compensated by myocyte proliferation in normal and hypoplastic fetal chick left ventricle. Circ Res. 2007; 100:1363–1370. [PubMed: 17413043]

Ergul A, Walker CA, Goldberg A, Baicu SC, Hendrick JW, King MK, Spinale FG. ET-1 in the myocardial interstitium: relation to myocyte ECE activity and expression. Am J Physiol Heart Circ Physiol. 2000; 278:H2050–2056. [PubMed: 10843904]

Gourdie RG, Harris BS, Bond J, Justus C, Hewett KW, O'Brien TX, Thompson RP, Sedmera D. Development of the cardiac pacemaking and conduction system. Birth Defects Research. 2003; 69C:46–57. [PubMed: 12768657]

Gourdie RG, Mima T, Thompson RP, Mikawa T. Terminal diversification of the myocyte lineage generates Purkinje fibers of the cardiac conduction system. Development. 1995; 121:1423–1431. [PubMed: 7789272]

Gourdie RG, Wei Y, Kim D, Klatt SC, Mikawa T. Endothelin-induced conversion of embryonic heart muscle cells into impulse-conducting Purkinje fibers. Proc Natl Acad Sci U S A. 1998; 95:6815–6818. [PubMed: 9618495]

Gurjarpadhye A, Hewett KW, Justus C, Wen X, Stadt H, Kirby ML, Sedmera D, Gourdie RG. Cardiac neural crest ablation inhibits compaction and electrical function of conduction system bundles. Am J Physiol Heart Circ Physiol. 2007; 292:H1291–1300. [PubMed: 17172273]

Hall CE, Hurtado R, Hewett KW, Shulimovich M, Poma CP, Reckova M, Justus C, Pennisi DJ, Tobita K, Sedmera D, Gourdie RG, Mikawa T. Hemodynamic-dependent patterning of endothelin converting enzyme 1 expression and differentiation of impulse-conducting Purkinje fibers in the embryonic heart. Development. 2004; 131:581–592. [PubMed: 14711873]

Hamburger V, Hamilton HL. A series of normal stages in the development of the chick embryo. J Morphol. 1951; 88:49–92.

Harris BS, Spruill L, Edmonson AM, Rackley MS, Benson DW, O'Brien TX, Gourdie RG. Differentiation of cardiac Purkinje fibers requires precise spatiotemporal regulation of Nkx2-5 expression. Dev Dyn. 2006; 235:38–49. [PubMed: 16245335]

Hewett KW, Norman LW, Sedmera D, Barker RJ, Justus C, Zhang J, Kubalak SW, Gourdie RG. Knockout of the neural and heart expressed gene HF-1b results in apical deficits of ventricular structure and activation. Cardiovasc Res. 2005; 67:548–560. [PubMed: 15907824]

Hunter AW, Barker RJ, Zhu C, Gourdie RG. Zonula occludens-1 alters connexin43 gap junction size and organization by influencing channel accretion. Mol Biol Cell. 2005; 16:5686–5698. [PubMed: 16195341]

Jafri F, Ergul A. Nuclear localization of endothelin-converting enzyme-1: subisoform specificity. Arterioscler Thromb Vasc Biol. 2003; 23:2192–2196. [PubMed: 14551152]

Kempf H, Linares C, Corvol P, Gasc JM. Pharmacological inactivation of the endothelin type A receptor in the early chick embryo: a model of mispatterning of the branchial arch derivatives. Development. 1998; 125:4931–4941. [PubMed: 9811577]

Kurihara H, Kurihara Y, Maemura K, Yazaki Y. The role of endothelin-1 in cardiovascular development. Ann N Y Acad Sci. 1997; 811:168–176. discussion 176-167. [PubMed: 9186595]

Kurihara Y, Kurihara H, Oda H, Maemura K, Nagai R, Ishikawa T, Yazaki Y. Aortic arch malformations and ventricular septal defect in mice deficient in endothelin-1. J Clin Invest. 1995; 96:293–300. [PubMed: 7615798]

Kurihara Y, Kurihara H, Suzuki H, Kodama T, Maemura K, Nagai R, Oda H, Kuwaki T, Cao WH, Kamada N, et al. Elevated blood pressure and craniofacial abnormalities in mice deficient in endothelin-1. Nature. 1994; 368:703–710. [PubMed: 8152482]

Nair S, Li W, Cornell R, Schilling TF. Requirements for Endothelin type-A receptors and Endothelin-1 signaling in the facial ectoderm for the patterning of skeletogenic neural crest cells in zebrafish. Development. 2007; 134:335–345. [PubMed: 17166927]

Pennisi DJ, Rentschler S, Gourdie RG, Fishman GI, Mikawa T. Induction and patterning of the cardiac conduction system. Int J Dev Biol. 2002; 46:765–775. [PubMed: 12382942]

Pikkarainen S, Tokola H, Kerkela R, Ilves M, Makinen M, Orzechowski HD, Paul M, Vuolteenaho O, Ruskoaho H. Inverse regulation of preproendothelin-1 and endothelin-converting enzyme-1beta

genes in cardiac cells by mechanical load. Am J Physiol Regul Integr Comp Physiol. 2006; 290:R1639–1645. [PubMed: 16410403]

Reckova M, Rosengarten C, deAlmeida A, Stanley CP, Wessels A, Gourdie RG, Thompson RP, Sedmera D. Hemodynamics is a key epigenetic factor in development of the cardiac conduction system. Circ Res. 2003; 93:77–85. [PubMed: 12775585]

Sedmera D, Hu N, Weiss KM, Keller BB, Denslow S, Thompson RP. Cellular changes in experimental left heart hypoplasia. Anat Rec. 2002; 267:137–145. [PubMed: 11997882]

Sedmera D, Pexieder T, Rychterova V, Hu N, Clark EB. Remodeling of chick embryonic ventricular myoarchitecture under experimentally changed loading conditions. Anat Rec. 1999; 254:238–252. [PubMed: 9972809]

Sedmera D, Reckova M, Bigelow MR, DeAlmeida A, Stanley CP, Mikawa T, Gourdie RG, Thompson RP. Developmental transitions in electrical activation patterns in chick embryonic heart. Anat Rec. 2004; 280A:1001–1009.

Takebayashi-Suzuki K, Yanagisawa M, Gourdie RG, Kanzawa N, Mikawa T. In vivo induction of cardiac Purkinje fiber differentiation by coexpression of preproendothelin-1 and endothelin converting enzyme-1. Development. 2000; 127:3523–3532. [PubMed: 10903177]

Tamaddon HS, Vaidya D, Simon AM, Paul DL, Jalife J, Morley GE. High-resolution optical mapping of the right bundle branch in connexin40 knockout mice reveals slow conduction in the specialized conduction system. Circ Res. 2000; 87:929–936. [PubMed: 11073890]

Wessels A, Markman MW, Vermeulen JL, Anderson RH, Moorman AF, Lamers WH. The development of the atrioventricular junction in the human heart. Circ Res. 1996; 78:110–117. [PubMed: 8603493]

Yanagisawa H, Hammer RE, Richardson JA, Williams SC, Clouthier DE, Yanagisawa M. Role of Endothelin-1/Endothelin-A receptor-mediated signaling pathway in the aortic arch patterning in mice. J Clin Invest. 1998a; 102:22–33. [PubMed: 9649553]

Yanagisawa H, Yanagisawa M, Kapur RP, Richardson JA, Williams SC, Clouthier DE, de Wit D, Emoto N, Hammer RE. Dual genetic pathways of endothelin-mediated intercellular signaling revealed by targeted disruption of endothelin converting enzyme-1 gene. Development. 1998b; 125:825–836. [PubMed: 9449665]

Yanagisawa M, Kurihara H, Kimura S, Tomobe Y, Kobayashi M, Mitsui Y, Yazaki Y, Goto K, Masaki T. A novel potent vasoconstrictor peptide produced by vascular endothelial cells. Nature. 1988; 332:411–415. [PubMed: 2451132]

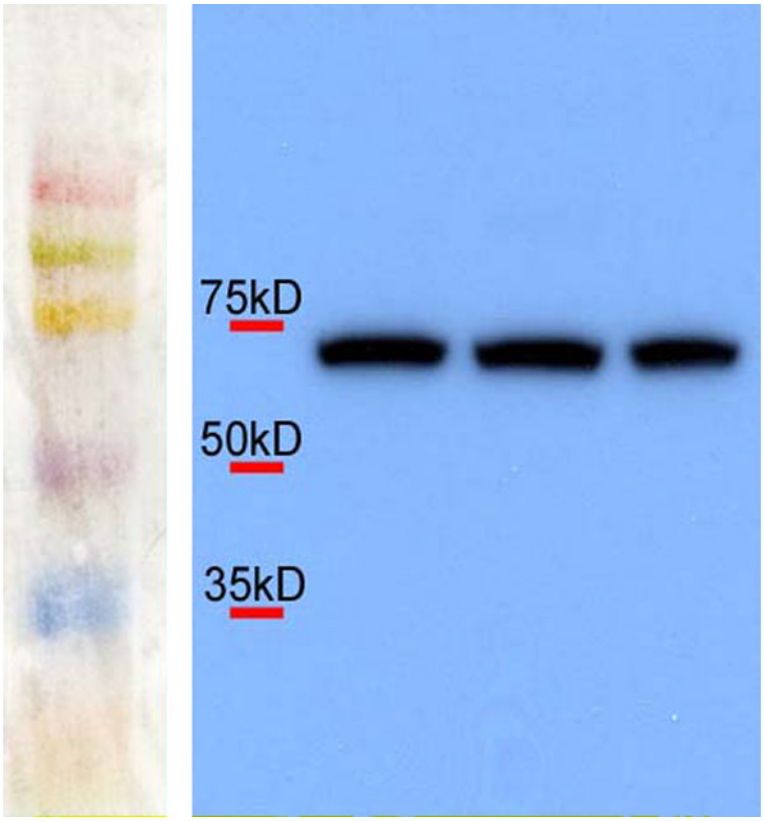

Figure 1.
Western blotting on homogenates from chick embryonic hearts. A single band is detected with the ECE antibody at ~70 kD. The individual lanes show results from three independent replicates.

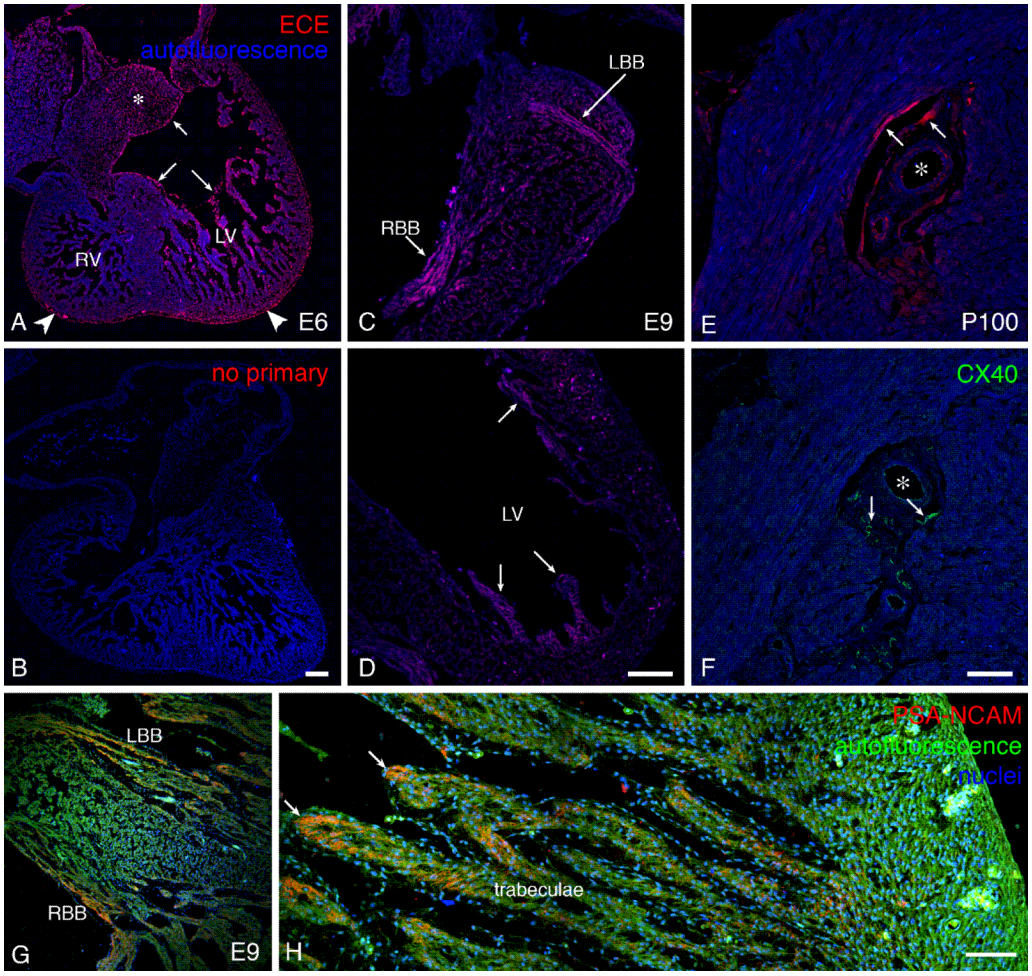

Figure 2.

Developmental profile of ECE expression in chick embryonic heart. A. At E6, the expression is mostly endocardial (arrows), but there is also positivity in the mesenchyme of the atrioventricular cushions (*) and epicardium (arrowheads). Omission of the primary antibody (B) results in no detectable staining. Scale bar 100 μm. C, D. At E9, expression becomes stronger in the myocardium, in particular in the forming CCS components (bundle branches in C, differentiating Purkinje fibers in the left ventricular apical trabeculae in D). Scale bar 100 μm. E. One hundred days after hatching, the expression in the coronary artery endothelium is prominent, and strong immunopositivity is also present in the periarterial Purkinje fibers. These areas correspond with expression of connexin40 on a sister section (F). Scale bar 50 μm. G, H: correlation with PSA-NCAM staining in an E9 embryo (compare with panels C, D). This antibody, used as a marker of developing conduction system, stains the bundle branches and tips of the trabeculae, i.e., areas of His-Purkinje system soon to become immuno-positive for connexin40. Scale bar in H 50 μm.

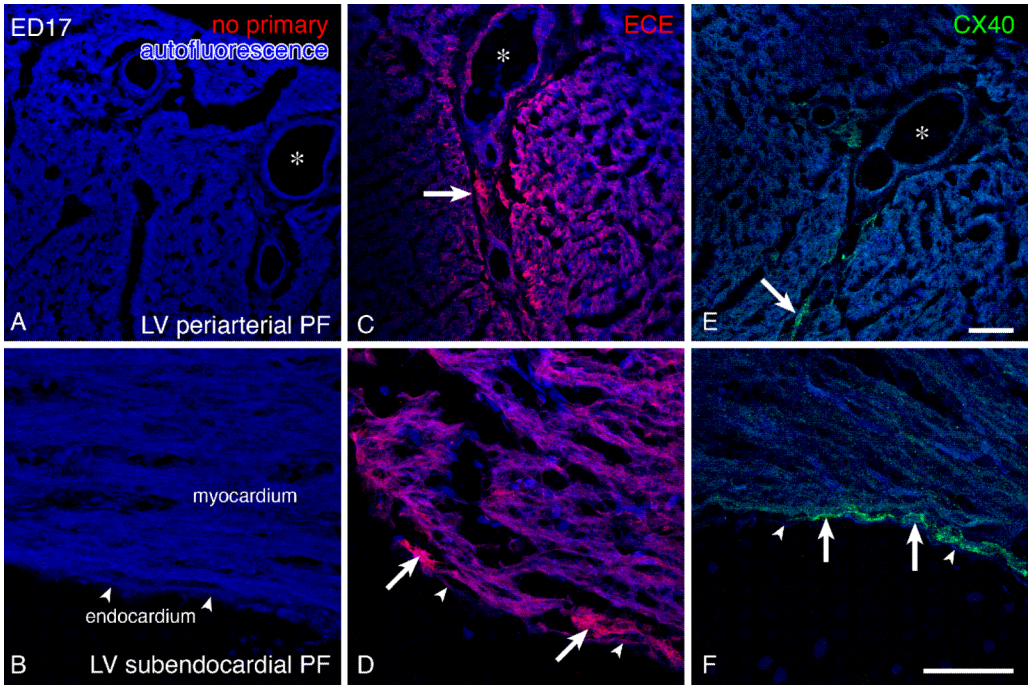

Figure 3.

ECE immunoreactivity in developing Purkinje fibers. Top row shows expression associated with the periarterial Purkinje fibers. No non-specific staining is observed with the omission of primary antibody (A). Coronary artery (*) endothelium is positive (C), and there is also strong expression in the periarterial Purkinje fibers (arrows), which rapidly decreases into the working myocardium. In contrast, connexin40 immunostaining performed on a sister section (E) is present only in the coronary artery endothelium and the Purkinje fibers, but not in the working ventricular myocardium. Scale bar (same for A, C, E) is 50 μm. Panels B, D, F show the same situation at higher magnification in the subendocardium. Endocardium is indicated by arrowheads. Scale bar 50 μm.

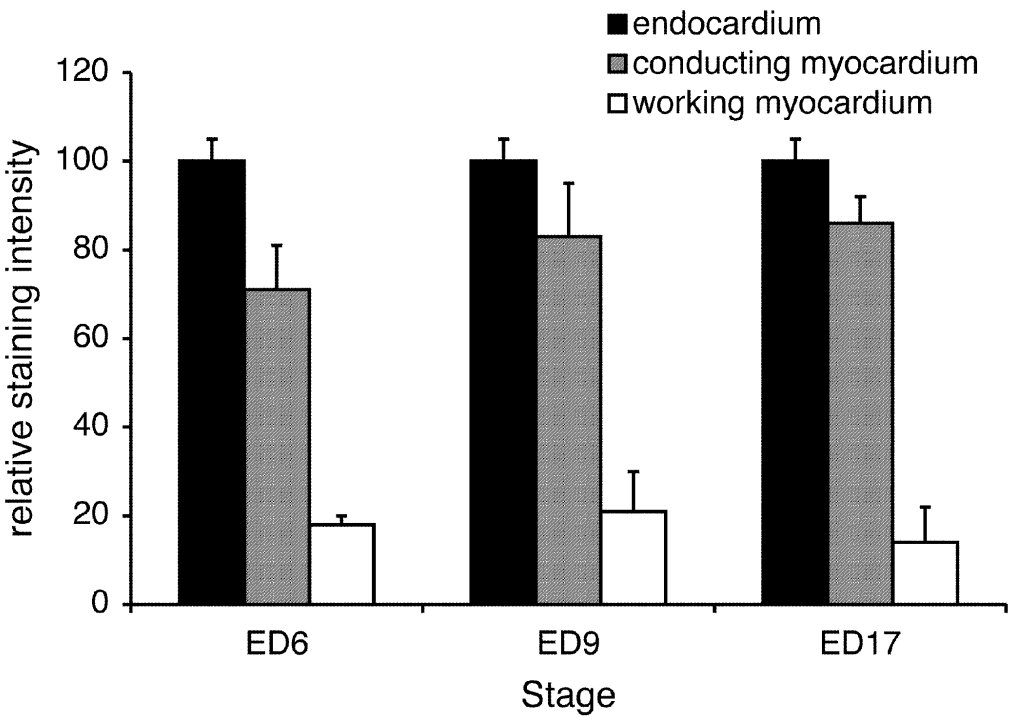

Figure 4.

Quantification of ECE staining intensity in different regions of the heart. The expression was consistently found to be the highest in the endocardium covering the atrioventricular valves, and the values in the conduction tissues exceeded those in the working myocardium. Maximum values from each compartment were used; the quantification is based on serial sections of at least 3 hearts per stage.

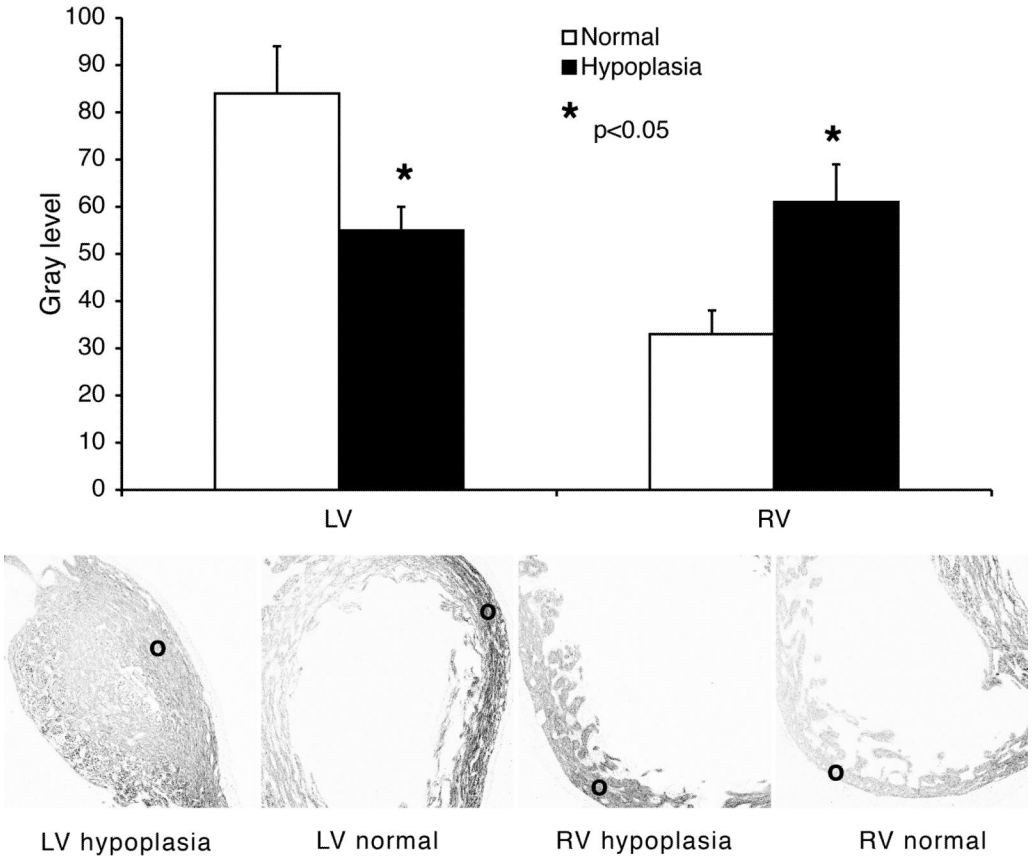

Figure 5.

Quantification of changes in ECE expression under experimentally altered hemodynamic conditions. There is a significant decrease in the left ventricle (LV) and an increase in the right ventricle (RV) in the experimental left heart hypoplasia group. Lower panels show typical examples of images taken from experimental and control hearts, with circles indicating the areas from which measurements were taken. Values are gray levels after background subtraction, mean ± SEM, n=12 per group, * $p<0.05$ (t-test).

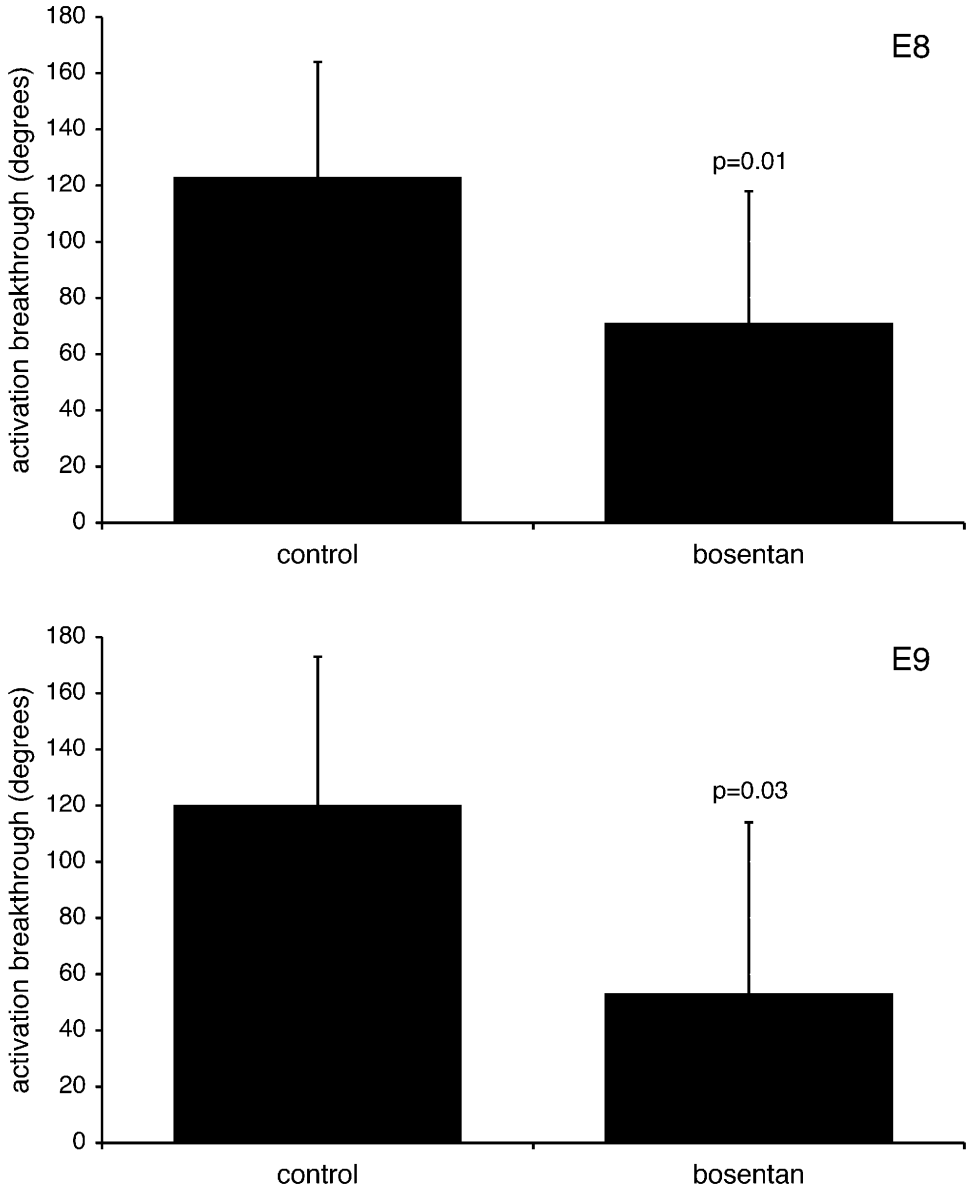

Figure 6.
Bosentan-induced delay of CCS maturation. Treatment with ET receptor antagonist results in decreased angle value of the epicardial breakthrough, a parameter that increases linearly with development from 50 to 150 degrees between Stages 29–35 (Gurjarpadhye et al., 2007).